

Size-Dependent Fate of Nanoceria in Large Scale Simulated Wetlands

by

Jane L. Cooper

Department of Civil and Environmental Engineering
Duke University

Date: _____

Approved:

Heileen Hsu-Kim, Co-Chair

Patrick Lee Ferguson, Co-Chair

Emily Bernhardt

Thesis submitted in partial fulfillment of
the requirements for the degree of
Master of Science in the Department of
Civil and Environmental Engineering in the Graduate School of
Duke University

2017

ABSTRACT

Size-Dependent Fate of Nanoceria in Large Scale Simulated Wetlands

by

Jane L. Cooper

Department of Civil and Environmental Engineering
Duke University

Date: _____

Approved:

Heileen Hsu-Kim, Co-Chair

Patrick Lee Ferguson, Co-Chair

Emily Bernhardt

An abstract of a thesis submitted in partial fulfillment of
the requirements for the degree of
Master of Science in the Department of
Civil and Environmental Engineering in the Graduate School of
Duke University

2017

Copyright by
Jane L. Cooper
2017

Abstract

Nanoceria, or cerium (IV) oxide, is used widely in industry for its catalytic and physical properties, thus its release into the environment is eminent. The environmental risk of nanoceria is still unclear, but understanding its environmental fate could help to inform future studies. To understand its fate, large scale simulated wetlands were constructed and dosed weekly. Nanoceria of primary particle sizes ~4nm (sm-CeO₂) and ~140nm (lg-CeO₂) were dosed into these mesocosms, 750 mg total over nine months. Single particle ICP-MS (spICP-MS) was employed with microsecond dwell times (0.1ms) to understand particulate cerium in surface water. spICP-MS proved ineffective as a comparison tool between treatments, since sm-CeO₂ was below instrument detection, and further data processing could not amend the issue. However, comparisons between nanoceria stocks and mesocosm samples could be conducted. Mesocosm water dosed with lg-CeO₂ exhibited some aggregation of its smaller fraction.

At the end of 9-months, elemental analyses showed that nanoceria size did not affect the mass of cerium in surface water, as mesocosms treated with lg-CeO₂ contained 4.0 ± 1.4 mg of Ce and sm-CeO₂ treated waters contained 5.6 ± 6.7 mg Ce. Greater biological uptake did occur when treated with smaller particles, as shown in elevated root concentration (sm-CeO₂: 67 ± 14 ng g⁻¹ ; lg-CeO₂: 21 ± 10 ng g⁻¹) and total Ce in *Egeria densa* biomass (sm-CeO₂: 22 ± 1.4 ; lg-CeO₂: 2.9 ± 0.5 mg). The environmental

compartments in this study accounted for a small fraction of dosed nanoceria (< 5%), so assumed nanoceria fate is the sediment.

Dedication

I dedicate this thesis to my partner, Michael, whose balance of logical thinking and sincere empathy gently inspired me when I needed it most. The recipe of Archer episodes, burrito bowls, and silliness helped me differentiate between mountains and mole hills.

I also dedicate this thesis to my family, Kathy, Andy, Ellen, and Jetta. Your unwavering love from miles away allowed me to jump into graduate school without hesitation, knowing I had your stable foundation supporting me all the while.

Finally, I dedicate this thesis to all the wonderful colleagues turned friends I met during my graduate school journey: Dean, Norm, Simone, Matt, Nicky, Brian, Amy, Lauren, Sarah, Ugonna, Dana, and more. You gave me a sense of community that counteracted those isolating days in lab, kept me laughing, and even turned me into a Duke Basketball fan.

Contents

Abstract.....	iv
List of Tables.....	ix
List of Figures.....	x
Acknowledgements.....	xi
1. Introduction.....	1
1.1 Chemistry of Cerium and Ceria.....	1
1.2 Nanoceria use and release.....	3
1.3 Fate and Transport of Nanoceria.....	5
1.4 Nanometrology.....	6
1.5 Research Objectives and Hypothesis.....	8
2. Materials and Methods.....	9
2.1 Wetland Mesocosm and Experimental Design.....	9
2.4 Sampling, Sample Preparation, Analyses.....	13
2.4.1 Total Cerium.....	13
2.4.2 Single Particle ICP-MS.....	15
2.4.3 Other Measurements.....	17
3. Results.....	18
3.1 Distribution of Nanoceria in Mesocosm Compartments.....	18
3.2 Particulate Cerium in Surface Water.....	20
3.2.1 Background Cerium.....	20

3.2.2 Mass of Cerium in Surface Water Particles.....	21
4. Discussion	25
4.1 Cerium Mass Balance.....	25
4.2 Applicability of Single Particle ICP-MS	26
5. Conclusions.....	29
Appendix A.....	30
Sample Collection.....	30
Appendix B	31
Mesocosm Sample Acid Digestion Protocol.....	31
Appendix C.....	32
Dosing Procedure	32
Appendix D.....	33
Mesocosm sampling plan.....	33
References	34

List of Tables

Table 1: Summary of organisms added to the wetland mesocosms, separated by zone.	11
---	----

List of Figures

Figure 1: The fluorite structure of stoichiometric Cerium(IV)Oxide, or ceria. Light spheres represent oxygen atoms, dark spheres represent cerium. If an oxygen left, two Ce(IV) atoms would reduce to Ce(III) to accommodate.	2
Figure 2: The regeneration mechanisms of surface cerium for the oxidation of peroxide via reduction by superoxide. From Celardo et al. ²⁰	5
Figure 3: Mesocosm dimensions and zone delineation. Each mesocosm is 1.2m by 3.7m. Aquatic zone sediment is fully submerged, while the degree of saturation in the transition zone depends on water level. Upland zone is kept above water level.	10
Figure 4: TEM Images of two nanoceria stocks. (A) Sm-CeO ₂ has an average diameter of 3.84 ± 1.13 nm; (B) Lg-CeO ₂ have an average diameter of 185.35 ± 63.71 nm.	12
Figure 5: Mass of cerium in surface water samples taken immediately before the weekly addition of 19.2 mg CeO ₂ nanoparticles. Data points refer to the average (± 1 std dev.) of 3 replicate mesocosm boxes. No significant difference between small and large treatments, but both are significantly different from the control mesocosm with no added cerium.	18
Figure 6 (a) Mass of cerium in Egeria and surface water. Ce in Egeria is greater in sm-CeO ₂ treatments than in lg-CeO ₂ and control (no Ce) treatments. (b) Concentration of cerium in Egeria roots is greater in small treatment mesocosms than other treatments.	20
Figure 8: Background equivalent diameter (BED) was elevated in mesocosms treated with small nanoceria. Large and control mesocosms were similar and matched the literature. ⁴⁶	21
Figure 9: (A) Nanoceria stock mass/particle distribution. (B) May mesocosm samples mass/particle. (C) June mesocosm samples mass/particle. (D) July mesocosm samples mass/particle.	23
Figure 10: Particle number concentration, in million particles per liter. Particle number concentration was suppressed in May compared to July, with variability in June between treatments (sm-CeO ₂ , lg-CeO ₂ , no-Ce).	24

Acknowledgements

I would first like to acknowledge my funding source:

- National Science Foundation (NSF) and the US Environmental Protection Agency (EPA) under NSF Cooperative Agreement EF-0830093, Center for the Environmental Implications of Nanotechnology (CEINT).

I gratefully acknowledge my advisors, Heileen “Helen” Hsu-Kim and Patrick “Lee” Ferguson and my lab-mates for generously spending your time teaching, helping, and mentoring. I want to especially thank Manuel Montaña for allowing me to apprentice with him in all things “nano”. Your creativity and deep understanding of the field made it a pleasure to work with you.

I’d also like to thank research collaborators within CEINT: Marie Simon and Steve Anderson (Duke University) for their organization and implementation of the CEINT mesocosms, Astrid Avellan (Carnegie Melon University) for biological analyses, Nicholas Geitner (Duke University) for nanoparticle characterization, Stella Marinakos (Duke University) for nanoparticle imaging, and Ben Colman (University of Montana) for your mesocosm guidance.

1. Introduction

The global market for cerium oxide nanoparticles, or nanoceria, was \$186 million in 2015, with more than half attributed to its use in catalysis and polishing. Nanoceria is also gaining popularity in personal care and cosmetic products, energy storage, and especially in biomedical sectors. By 2022, the market is expected to quadruple, with largest growth in the biomedical application.¹ With this explosion in use across industries comes a heightened threat of environmental release, yet the environmental risk of nanoceria is uncertain. Understanding the ultimate environmental fate of these nanoparticles is crucial to properly assess risk before particles become omnipresent.

1.1 Chemistry of Cerium and Ceria

Cerium is a naturally occurring element, with a mass of 140 amu electronic configuration of $4f^25d^06s^2$. Though classified as a rare-earth element (REE), cerium is the 26th most common element in the Earth's crust at 66 ppm, just behind copper at 68 ppm. Monazite ($Ce,LaPO_4$) and Bastnasite ($REE-CO_3F$) are the two most commonly mined cerium-containing minerals, though one can find cerium in many others.

Cerium(IV) and oxygen form a dioxide commonly called ceria (CeO_2) [Fig1].² In low oxygen or high temperature conditions, ceria deviates from its dioxide stoichiometry CeO_{2-y} where ($2 > y > 0.5$). Two Ce(IV) atoms reduce to Ce(III) when oxygen leaves. This oxidation-reduction (redox) behavior accommodates the excess electrons, but causes defects in its regular fluorite structure³. This redox ability is

reversible and repeatable, and oxygen vacancy defects can migrate within the crystal structure. These two properties of ceria allow for a high oxygen storage capacity (OSC), material to be an effective catalyst.³

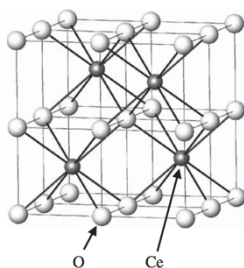


Figure 1: The fluorite structure of stoichiometric Cerium(IV)Oxide, or ceria. Light spheres represent oxygen atoms, dark spheres represent cerium. If an oxygen left, two Ce(IV) atoms would reduce to Ce(III) to accommodate.

In a ceria unit cell, cerium is coordinated with 8 oxygen atoms in a fluorite structure (Figure 1). A collection of these unit cells can form a ceria nanoparticle, or nanoceria for the this article⁴ To be classified as a nanoparticle (NP), it must have at least two dimensions between 1 and 100nm. NPs usually exhibit enhanced or new found reactivity in comparison to their bulk form⁵. Higher specific surface area means a greater proportion of cerium on the particle surface and susceptible to redox activity.

Other governing physicochemical properties include its relative insolubility and softness. Bare particles exhibit an isoelectric point at pH 8 in deionized water.⁶

Nanoceria can be synthesized via numerous methods, such as , each producing particles with unique crystal morphologies, ranges in diameter, crystal facets with varying surface chemistry, and finished with a selection of coatings or stabilizers⁷⁻⁸.

1.2 Nanoceria use and release

The intrinsic hardness and reactivity of CeO₂-NPs is utilized as an abrasive in chemical-mechanical polishing and planarization (CMP). CMP is the middle ground between chemical etching and mechanical abrasion, minimizing both scratching and corrosion⁹. The microelectronics industry and glass producers, among others, employ a slurry including CeO₂, Al₂O₃, and SiO₂ for their CMP process. The average particle used in CMP is between 20 and 200 nm, with primary particle sizes approaching <100nm.¹⁰ Literature shows removal of CeO₂ from water in traditional waste water treatment plants (WWTP)¹¹⁻¹³, but there is less information on the efficacy of water treatment processes at onsite facilities at industrial sites.¹⁰

Redox activity of nanoceria and its resulting OSC make it an effective catalyst. Another growing application of nanoceria is as an additive in diesel fuel. Nanoceria enables three-way catalysis (TWC) reactions that, among other effects, stores and releases oxygen during the combustion process and thereby reducing the emission of carbon monoxide (CO), nitrous oxide (NO_x), and unburnt hydrocarbons (HCs).¹⁴ Though filters collect some ceria-soot particles in the exhaust gas, studies show release of agglomerates of soot-nanoceria into the atmosphere¹⁵⁻¹⁷. Models have shown the additive nanoceria increases in diameter from <10 nm to ~100 nm during combustion.¹⁸ Eventual deposition would introduce nanoceria into the terrestrial environment, with little knowledge of its eventual fate.¹⁷

Biomedical research utilizes nanoceria for its biomimetic chemistry. The reversible redox activity of these NPs mimics two enzymes, superoxide dismutase and catalase, exhibiting antioxidant and oxidant behavior, respectively [Fig2]¹⁹⁻²⁰. Surface redox regeneration has been shown in nanoceria, allowing for prolonged efficacy. Complete control of these behaviors is still an aspiration in biologically relevant conditions, but nanoceria show promise as a therapeutic for multiple sclerosis²¹, age-related macular degeneration²² and diabetic retinopathy.²³ Its biopersistence and nonspecific and rare application make environmental release hard to predict. Nanoceria used in biomedical applications have to cross cell membranes, thus particles <50 nm are used, with trends towards smaller sizes²⁴. Human waste will enter WWTPs and undergo effective NP removal¹¹⁻¹³, but possible improper disposal of therapeutics leaves room for nanoceria environmental release into any environmental compartment.

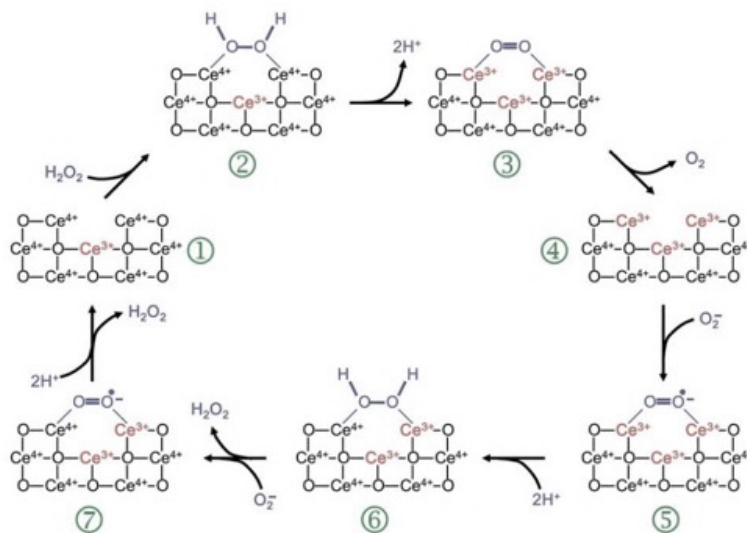


Figure 2: The regeneration mechanisms of surface cerium for the oxidation of peroxide via reduction by superoxide. From Celardo et al.²⁰

1.3 Fate and Transport of Nanoceria

The environmental risks of engineered nanoparticles depend in part on the distribution and transformation of the nanoparticles after their release to the environment. Aggregation may decrease the toxicity of nanoceria, due to a decrease in reactive surface area. Reactive oxygen species (ROS) are generated on particle surfaces, so aggregation would limit the production of such cytotoxic species.²⁵ As such, aggregation is often a focus in the nano-risk research community due to its importance for determining the environmental fate of nanoceria. Other processes such as dissolution are not a great concern, as ceria is generally insoluble above pH 4.

Derjaguin, Landau, Verwey, and Overbeek (DLVO) theory is often used to model nanoparticle aggregation in environmental matrices, as reviewed in depth by Hotze *et al.*²⁶ Briefly, DLVO describes the balance of van der Waals attraction and electrostatic repulsion between two particle surfaces. An attachment event (i.e. aggregation) occurs when attraction overcomes repulsion, either between the same particles (homoaggregation) or those of different composition (heteroaggregation). With aggregation, effective particle size increases, which subsequently changes its mobility, reactivity, and toxicity²⁷. Particles may grow large enough to settle out of the water column (Stoke's Law)²⁶. However, DLVO-based models cannot yet predict nanoceria

aggregation, as they exclude many crucial variables from aquatic environments and nanoparticle chemistry.

Many researchers have shown in practice that nanoceria aggregation is controlled by the aquatic variables: ionic strength,²⁸ pH,²⁹ and presence of natural organic matter (NOM),^{6, 28} natural colloids,³⁰⁻³² ligands,^{29, 31, 33} and certain electrolytes³⁴ – with some conflicting conclusions. Compounded on these results, it was found that particle coating and initial size also contribute to the degree of aggregation, among other variables associated with synthesis.³⁵⁻³⁷

1.4 Nanometrology

Since the aquatic fate of NPs is determined largely by aggregation and sedimentation, any studies on the environmental implications of NPs generally require nanometrology to capture additional characteristics beyond mass concentration, such as NP size, number, and aggregation state. Many conventional analytical techniques are inadequate in application to NP studies in environmental media, described in depth by Baalousha et al.³⁸⁻³⁹. For example, atomic force microscopy (AFM) and electron microscopy (EM) are extremely time intensive and do not allow for analysis of many samples. EM sample preparation requires a drying step under vacuum that may alter NP aggregation state, while AFM can introduce instrumental and environmental artefacts. Dynamic light scattering (DLS) is a faster technique with little sample preparation, but loses accuracy in solutions of both low and high particle concentration,

broad size distributions, and with non-spherical particles. These limitations preclude effective application of DLS for many environmental waters.

Elemental analysis such as inductively coupled plasma – mass spectrometry (ICP-MS) provides total metal concentration at environmentally relevant concentrations, and commonly handles high sample throughput. However, conventional ICP-MS data alone does not provide information about particle characteristics in environmental systems. Particle separation methods (e.g. filtration, centrifugation) have been used to discern particulate and dissolved species. However, these methods are operationally defined based on filter size and material. Another challenge with elemental analyses is they cannot delineate between background and engineered nanoparticle metal contributions.

Single particle ICP-MS (spICP-MS) supplements traditional ICP-MS by providing particle size distribution, particle number concentration, and particle mass.⁴⁰ Many studies have shown spICP-MS to be a valuable tool in measuring nanoparticles accurately, and in complex matrices.⁴¹⁻⁴⁴ However, nanoceria introduces difficulties in with its synthesis-associated polydispersity. When two particles are measured together, data processing mistakes them as one particle event, a phenomenon referred as particle coincidence. Monodisperse particles have a consistent average signal, so if this signal doubles due to the presence of two particles, coincidence is assumed and accounted for as two particles. Polydisperse solutions have a wide range of particle sizes, and a range

of associated particle signals, making coincidence detection and deconvolution more difficult.⁴⁵ Decreasing instrument dwell time from 3 ms to 0.1 ms has shown to reduce coincidence, but the lower end of polydisperse particle distributions can still blend into background noise. Therefore, a statistically defined background truncates a solution's the full particle distribution.⁴⁵ Despite its polydispersity, the fundamentally low background of dissolved ceria allows for a low size detection limit (~10nm).⁴⁶

1.5 Research Objectives and Hypothesis

Researchers have previously employed aquatic mesocosms to study mechanisms governing the fate of nanoceria and the effects of surface coatings³⁵⁻³⁶. These experiments provide insight into short term nanoceria fate (e.g. 4 weeks), but the indoor controlled setups lacked the complexity in biota, scale, and seasonality of to truly mirror a natural environment. This study aims to understand the environmental fate of nanoceria within a vegetated wetland mesocosm ecosystem over the span of several months, and to study the relevance of primary particle size in controlling concentration in the surface water compartment that is a major conduit for biological exposure. The feasibility of spICP-MS techniques was also tested to further understand nanoceria fate in simulated wetlands waters where particle polydispersity, particle size detection limit, and natural cerium occurrence were considered in the analysis.

2. Materials and Methods

2.1 Wetland Mesocosm and Experimental Design

Outdoor aquatic mesocosms were constructed in the Duke Experimental Forest, in Durham, NC and designed to mimic freshwater, vegetated wetlands. Previous studies have established the mesocosm designs.⁴⁷ In brief, the rectangular boxes were constructed of treated wood, with the bottom sealed with a geotextile (0.45 mm reinforced polypropylene, Firestone Specialty Products, U.S.) and dimensions of 0.81m high, 1.22m wide, and 3.66m long [Fig 3]. Mesocosms consisted of three zones: aquatic, transition, and upland. All zones were covered with soil the texture class sandy-loam with 19.6% clay, 24.3% silt, and 56.1 sand size fractions, with a 13° incline starting at the aquatic-transition zone delineation. Bulk density for the floc, aquatic, and upland sediment were 0.08, 1.14, and 1.16 g cm⁻³ respectively. The aquatic zone was always submerged in water, while water levels control saturation of the transition zone, and the upland zone was never inundated. Water was sourced from a well at the mesocosm facility in the Duke Experimental Forest. A greenhouse covered the mesocosms only for the first two months of the experiment, and mesocosms were subsequently left open to the environment.

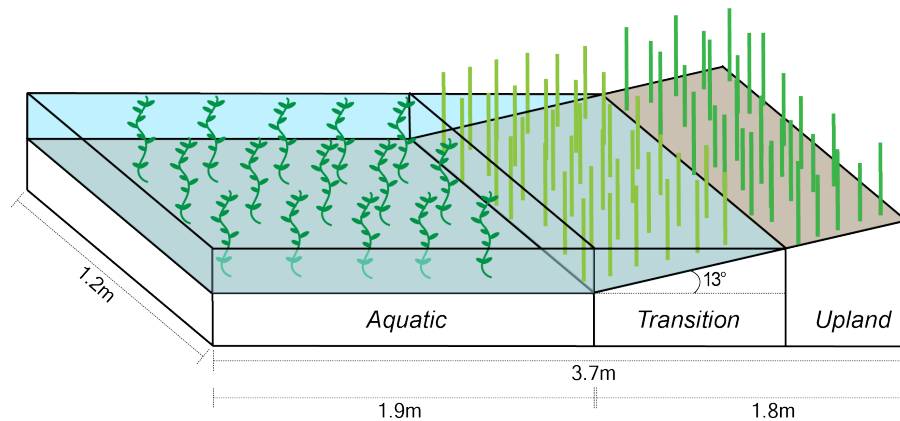


Figure 3: Mesocosm dimensions and zone delineation. Each mesocosm is 1.2m by 3.7m. Aquatic zone sediment is fully submerged, while the degree of saturation in the transition zone depends on water level. Upland zone is kept above water level.

The mesocosms were planted in June 2015, in a non-randomized design [Table 1]. In brief, *Egeria densa*, or Brazilian waterweed, cuttings were planted in the aquatic zone in a three by five grid. Transition zone was planted with plugs of Shallow sedge (*Carex lurida*), Cardinal flower (*Lobelia cardinalis*), and Soft rush (*Juncus effuses*). Upland soils were introduced to plugs of Switchgrass (*Panicum virgatum*) and River oats (*Chasmanthium latifolium*), and seeded with Annual ryegrass (*Lolium multiflorum*) and Big bluestem (*Adropogen gerardii*). Biweekly inoculums of phytoplankton and zooplankton were added, sourced from a local wetland. Other non-plant organisms in the mesocosms, henceforth referred to as organisms, include: Eastern mosquitofish (*Gambusia holbrooki*, Triangle Pond Management), freshwater snails (*Physella sp.* and *Lymnaea sp.*), Asiatic clams (*Corbicula fluminea*, West Point on the Eno). Snails were introduced unintentionally, transplanted with *Egeria* cuttings but efforts were made to

distribut them evenly between boxes prior to NP addition. Clams did not survive the experiment, and were removed 149 days into the experiment. Miscellaneous benthic macroinvertebrates, such as chironomids, damselflies, and dragonflies, colonized the mesocosms naturally.

Table 1: Summary of organisms added to the wetland mesocosms, separated by zone.

Zone	Aquatic	Transition	Upland
Flora	<i>Egeria densa</i> <i>Juncus effuses</i> <i>Poramogeton diversifolious</i> ^a	<i>Carex lurida</i> <i>Lobelia cardinalis</i>	<i>Panicum virgatum</i> <i>Chasmanthium latifolium</i> <i>Lolium multiflorum</i> ^b <i>Andropogen gerardii</i> ^b
Fauna	<i>Gambusia holbrooki</i> ^c Snails (<i>Physella sp.</i>) <i>Corbicula fluminea</i> ^d Misc. benthic macroinvertebrates Inoculum of phytoplankton + zooplankton ^e		
^a Accompanied the <i>J. effuses</i> ; ^b Most upland portion; ^c From Triangle Pond Management; ^d From Eno River, in floats 10-15cm from surface; ^e Added biweekly leading up to experiment start and throughout experiment, and sourced from local wetland.			

Two nanoceria stocks of different average sizes were used for the mesocosm experiments. The nominally small CeO₂ NPs (Sm-CeO₂) was stabilized in acetate (Nyacol CeO₂AC-30, 29%w/w in H₂O). They had a primary particle size of 3.84 ± 1.13 nm, as determined by TEM [Fig4A]. The large CeO₂ particles (Lg-CeO₂) exhibited increased polydispersity, relative to its smaller counterpart, with an average diameter of

185.35 ± 63.71 nm [Fig4B]. This NP was stabilized in an unknown, proprietary dispersant (Alfa Aesar NanoArc Ce-6080, 11% w/w in H₂O). Suspended in mesocosm water, the sm-CeO₂ has a positive zeta potential (+35.2 ± 6.5 mV), and lg-CeO₂ exhibits negative surface charge (-10.7 ± 4.5). For reference, bare nanoceria have an isoelectric point at pH 8, whereas the sm-CeO₂ stock pH is 3 and lg-CeO₂ was not measured.

Each type of CeO₂ (small and large) was added to triplicate mesocosm boxes, and three additional boxes with no added CeO₂ were monitored as controls. Nanoparticles were added to the surface water of mesocosms starting on January 18, 2016 with 19.2 mg Ce from the respective CeO₂ stock suspension. This dose corresponded to an approximate concentration of 0.045 mg L⁻¹ in the mesocosm surface water (depending on water level). This same dose of nanoceria was added once every seven days for a cumulative 750 mg of cerium over nine months.

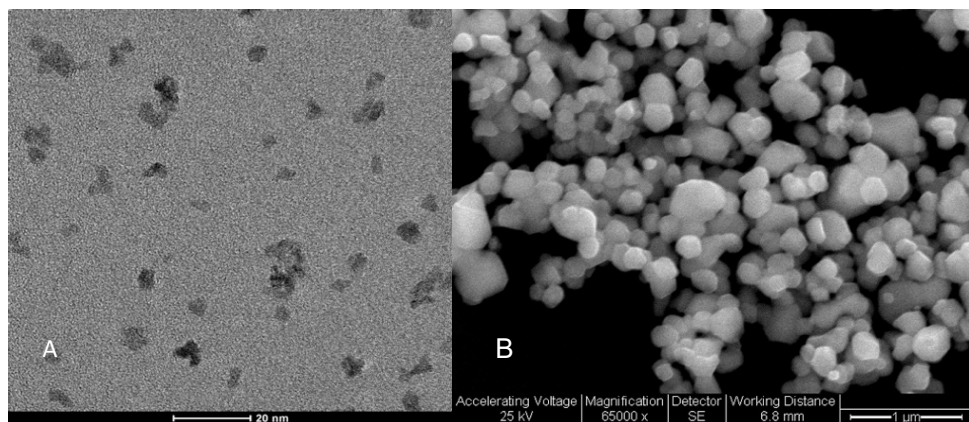


Figure 4: TEM Images of two nanoceria stocks. (A) Sm-CeO₂ has an average diameter of 3.84 ± 1.13 nm; (B) Lg-CeO₂ have an average diameter of 185.35 ± 63.71 nm.

2.4 Sampling, Sample Preparation, Analyses

2.4.1 Total Cerium

Unfiltered surface water was collected on a weekly basis, immediately before the weekly dose of nanoceria to the surface water. This water was acidified in field, and digested further in the laboratory.

Samples of flora were collected quarterly (3-, 6-, and 9-month time points) for cerium content. *Egeria* was collected within a constant vertical cylinder in the aquatic zone (n=4), referred to as “stovepipe”, from the water level to the sediment surface. This technique gives a representative sample of *Egeria* at all depths. All plant biomass harvest in the stovepipe were rinsed with water, resulting in the removal of loosely bound periphyton and weakly adsorbed nanoparticles. *Egeria* samples were freeze dried, ground, and digested before ICP-MS analysis. Total biomass was determined by harvesting all *Egeria* in the mesocosm at the experiment’s culmination at 9 months. A subset of *Egeria* roots and stems were also collected, but those lack associated biomass data. Roots are buried in the sediment, therefore not included in the stovepipe *Egeria*. Stems are included in the stovepipe samples, but they were separately analyzed to determine concentration in new growth in the photosynthetic range of the water column. No mass balance analysis was conducted on these samples.

Sediment cores were collected quarterly from the aquatic, transition and upland zones of each mesocosm. Aquatic and transition zone cores were 1 cm in depth,

whereas upland cores were 5cm. Flocc, or the organic rich layer of detritus hovering over the sediment, was also collected in the aquatic zone. Sediment cores were collected in triplicate from each zone of each mesocosm and homogenized before analysis. Splits of these samples were used to determine sediment bulk density. Others underwent microwave digestion prior to total metal analysis by ICP-MS.

Elemental analysis of the sediment samples was performed by microwave-assisted acid digestion, whereas *Egeria* and surface water samples used hot block digestion (3:3:1 ratio of nitric acid, hydrochloric acid, and hydrogen peroxide). The digested samples were then diluted and then analyzed for a suite of metals, including cerium(Ce), lanthanum (La), neodymium (Nd) with ICP-MS (Agilent Technologies 7900). Ce mass in the surface water was determined by multiplying aqueous concentration and the water volume (as determined by water level measurements and the geometry of the mesocosm box). Ce mass in plants was calculated by the mass concentration multiplied by total plant biomass, as determined at the 9-month harvest. Total Ce mass in sediment was calculated assuming the measured sediment sample represented the top 1 cm layer of sediment, or 5 cm for upland soils.

Analysis of Variance was utilized to determine significance between treatments ($\alpha = 0.05$). Paired t-test was applied to determine size dependent differences in weekly surface water data ($\alpha = 0.05$).

2.4.2 Single Particle ICP-MS

Unfiltered surface water was collected monthly for analysis via spICP-MS (Agilent 7900). The sample was run within 24 h of sampling, without any pretreatment, dilution, or sonication. Instrument sample introduction rate was 0.35 ml min^{-1} and samples had 60 seconds of data collection with 0.1ms dwell times between data points. Oxides (156/140) and doubly charged oxides (70/140) were confirmed under 3% prior to analyses and transport efficiency remained between 7-12%.

Raw data of intensity (counts) over time was converted to mass per particle event using methods outlined by Pace et al.⁴⁸ Briefly, transport efficiency (η_n) was determined by adjusting it until calculated diameter of a monodisperse standard NP (NIST 8013) equaled its certified size. Then the raw spICP-MS data for the mesocosm samples were analyzed first for background intensity (I_{Bkgd}) of Ce. This baseline intensity value was determined in each sample through an iterative process in which the average intensity (μ) plus 3 standard deviations (σ) of the data were used to filter out outlier values (e.g. discrete CeO₂ particles), followed by a new $\mu + 3\sigma$ threshold to filter remaining data, repeated until no data points remain above the final filter ($\mu + 3\sigma$). The signal intensity at this threshold was then defined as the background signal, I_{Bkgd} , and peak signals over this threshold were designated particle intensities (I_p). The lower limit of detectable particle size increases with higher values of I_{Bkgd} . To further eliminate background noise, an additional filter required that a particle event last at least 0.2ms.

Dissolved standards provided metrics to relate I_p to mass concentration. The concentration of dissolved standards (C ; 0, 1, 2, 5, 10 ng Ce mL⁻¹) was converted to mass flux (W ; ng Ce × particle⁻¹) via Eq.1. A linear regression between W and I_p was determined, providing the variables of slope (m) and intercept (b) to relate instrument response to Ce mass. Those variables were used as variables in Eq.2, which converted the intensity of particle events (I_p) to mass per particle event (m_p).

$$W = \eta_n \times q_{liq} \times t_{dwell} \times C \quad (1)$$

$$m_p = \frac{1}{f_a} \frac{(I_p - I_{bkgd}) \times \eta_i - b}{m} \quad (2)$$

Dwell time (t_{dwell}) refers to the time over which data is integrated, and 0.1ms are employed in this study. The mass fraction (f_a) of nanoceria is 0.81, assuming a perfect dioxide structure. The ionization efficiency (η_i) of Ce in is approximately 1.

To understand the limits of particle detection due to background signal, one can calculate the background equivalent diameter (BED), or background equivalent mass. The diameter of a particle is calculated in Eq. 3, assuming spherical particles and constant density (ρ_p), and by fitting a log-normal curve. To find BED, use the iterative background 3σ as I_p in Eq.2 and Eq.3.

$$D_p = \sqrt[3]{\frac{6 \times m_p}{\pi \times \rho_p}} \quad (3)$$

Particle number concentration (N_p) is calculated with by counting particle events (Eq.4), where q_{liq} denoted sample uptake rate (3 mL min^{-1}). This metric provides more information to understand the given nanoparticle sample, and rate of coincidence.

$$N_p = \frac{\Sigma(I_p)}{q_{liq} \times \eta_n} \quad (4)$$

2.4.3 Other Measurements

In situ aquatic measurements (pH, temperature, turbidity, conductivity, and dissolved oxygen) and nutrient levels (NO_3^- , SO_4^{2-} , ortho- PO_4) were collected weekly by Eureka and YSI multi-probe. Precipitation data was also collected on site.

3. Results

3.1 Distribution of Nanoceria in Mesocosm Compartments

Each mesocosm box was examined for partitioning of Ce into major compartments, including the surface water, surface sediment, and submerged plant biomass (i.e. *Egeria*) in the aquatic zone. Cerium generally did not accumulate in surface water, as shown the relatively constant mass of Ce in the surface water compartment over the 9-month experiment [Fig 5]. There was no difference in Ce between sm-CeO₂ and lg-CeO₂ treated mesocosm surface waters, but both were significantly greater than the controls. Total cerium mass remained below 20 mg for most of the nine months, with few outliers. Those outliers on March-14, April-4 and June-20 came with large variation between mesocosm triplicates. That variability is not present in control mesocosms.

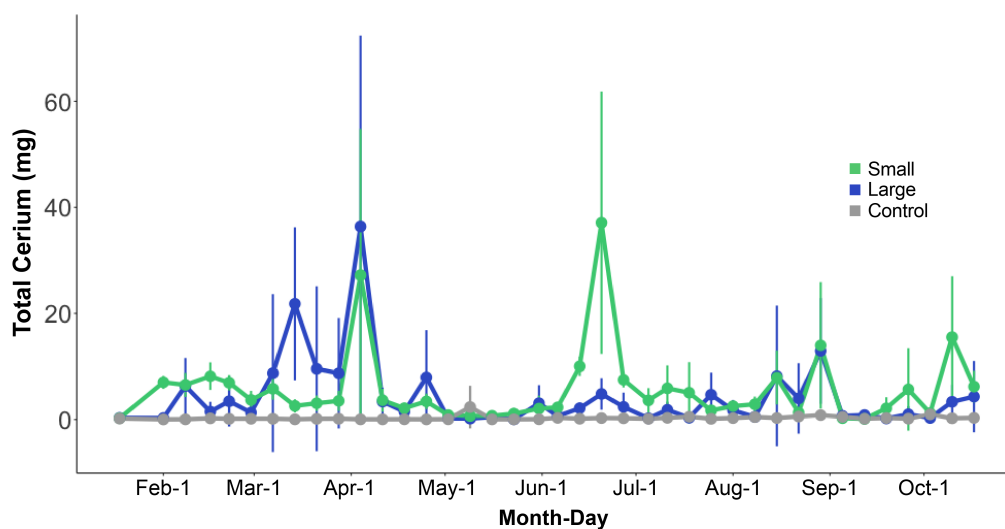


Figure 5: Mass of cerium in surface water samples taken immediately before the weekly addition of 19.2 mg CeO₂ nanoparticles. Data points refer to the average (± 1 std dev.) of 3 replicate mesocosm boxes. No significant difference between small and

large treatments, but both are significantly different from the control mesocosm with no added cerium.

Cerium contents varied with particle size in biological compartments of the mesocosms, but did not affect not surface water Ce content at the end of the 9-month experiment. In mesocosms dosed with sm-CeO₂, rinsed *Egeria* accumulated 22 ± 1.4 mg of Ce, and seven times more Ce than *Egeria* in the lg-CeO₂ (2.9 ± 0.5 mg) while the accumulation of Ce in the *Egeria* compartment of the no-Ce controls was 1.6 ± 0.5 mg total Ce. Total Ce in *Egeria* samples were all greater than the respective rinsed samples (as expected), but the difference between total Ce mass on *Egeria* in the sm-CeO₂ mesocosms (31 ± 4.3 mg) were only 3.5 times greater than Ce on unrinsed *Egeria* of the lg-CeO₂ treatments (8.4 ± 4.5 mg).

Ce in the *Egeria* roots exhibited more than 3 times the Ce concentration that *Egeria* roots in sm-CeO₂ treated mesocosms (sm 67 ± 14 ng g⁻¹ vs. lg 21 ± 10 ng g⁻¹). Stem Ce concentrations are negligible across in both sm-CeO₂ (1.4 ± 0.7 ng g⁻¹) and lg-CeO₂ (0.24 ± 0.22 ng g⁻¹).

As outlined by the weekly data, surface water Ce mass was not significantly affected by NP addition (lg-CeO₂: 4.0 ± 1.4 ; sm-CeO₂: 5.6 ± 6.7 mg). Mass of Ce in sediment, transition and upland biota, and other organisms have yet to be reported.

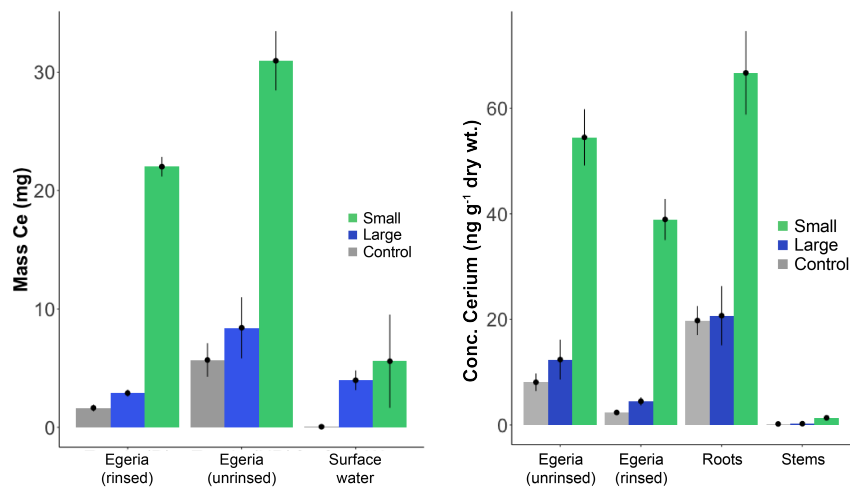


Figure 6 (a) Mass of cerium in Egeria and surface water. Ce in Egeria is greater in sm-CeO₂ treatments than in lg-CeO₂ and control (no Ce) treatments. (b) Concentration of cerium in Egeria roots is greater in small treatment mesocosms than other treatments.

3.2 Particulate Cerium in Surface Water

3.2.1 Background Cerium

In the sp-ICPMS analysis, the baseline signal intensity, as expressed by BED value, was elevated in the surface water of mesocosms treated with sm-CeO₂ in comparison to the other treatments and the NP stocks [Fig 8.] In those mesocosms, the BED in May, June, and July were 86.5nm, 240.4nm, and 75.8nm respectively. High BED resulted in elevated minimum detectable Ce particle mass in waters treated with sm-CeO₂, which removed all smaller particle events.

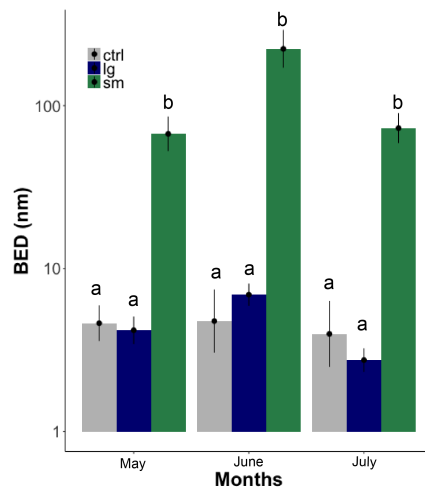


Figure 7: Background equivalent diameter (BED) was elevated in mesocosms treated with small nanoceria. Large and control mesocosms were similar and matched the literature. ⁴⁶

3.2.2 Mass of Cerium in Surface Water Particles

Since sm-CeO₂ dosed mesocosm waters exhibited high background levels, direct comparisons cannot be made between the two NP treatments. However, compared to its own stock diluted solution, sm-CeO₂ Ce mass per particle distributions appear have shifted to larger values one suspended in the mesocosm water. The average mass per particle event in those mesocosms centered around 10⁻⁶–10⁻⁴ ng while the sm-CeO₂ stock solutions were 10⁻⁸–10⁻⁵ ng per particle event.

Control and large treatments had similar BED values, so comparison between the natural Ce-containing particles and lg-CeO₂ was permissible [Fig. 8]. Lg-CeO₂ treated waters ranged between 10⁻⁷–10⁻³ ng/particle event, whereas its stock also included smaller particles (10⁻⁹–10⁻³ ng/event). Control mesocosms contained comparatively less large

particles (10^{-7} - 10^{-4} ng/event), but not statistically different from lg-CeO₂ mesocosms in July [Fig. 8].

Particle number concentration (#/liter) in all treatments are relatively similar, except for June sm-CeO₂ mesocosms, which are significantly concentrated [Fig 10]. Average particle concentration for lg-CeO₂ mesocosms remained between $1-2 \times 10^6$ particles per liter, whereas July surface waters increased in concentration to $3-4 \times 10^6$. By July, all three treatments contained a similar number of particles.

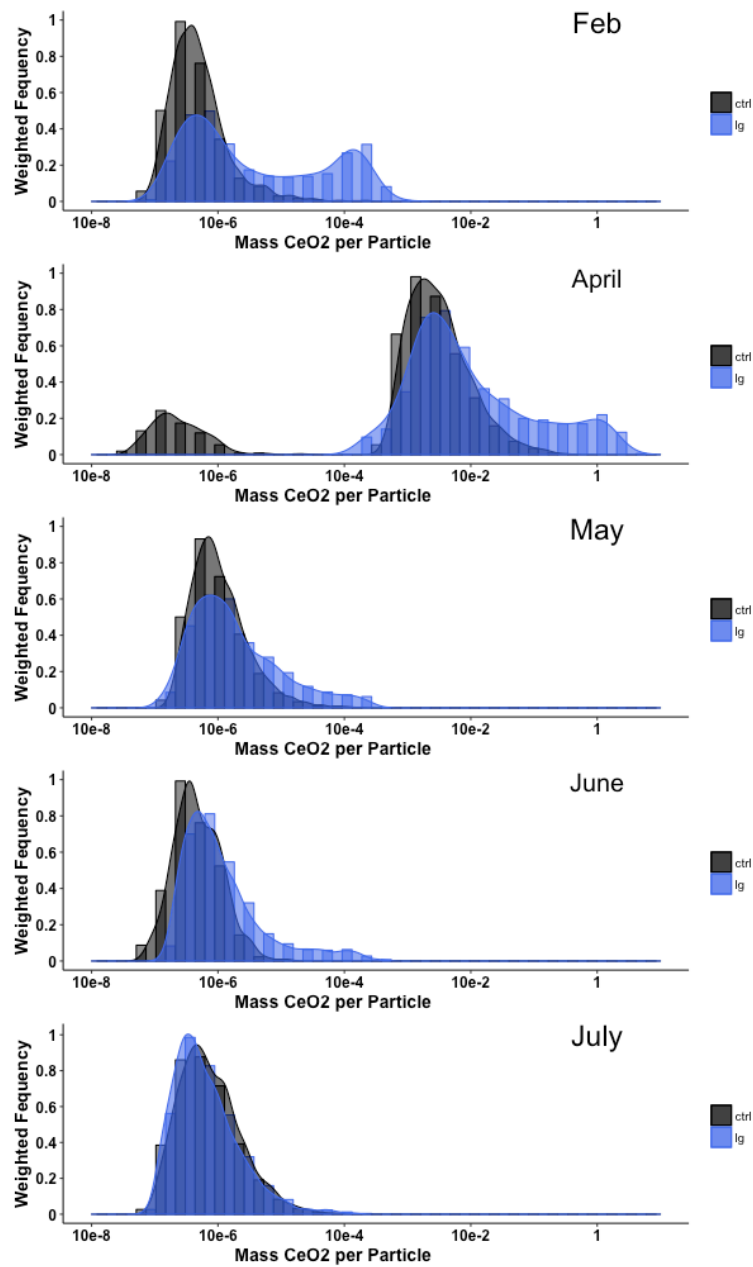


Figure 8: Distribution of particle mass in lg-CeO₂ and no-CeO₂ treated mesocosms over time. Distributions shift to larger values in April. By May, mass distribution mimics that of natural NPs.

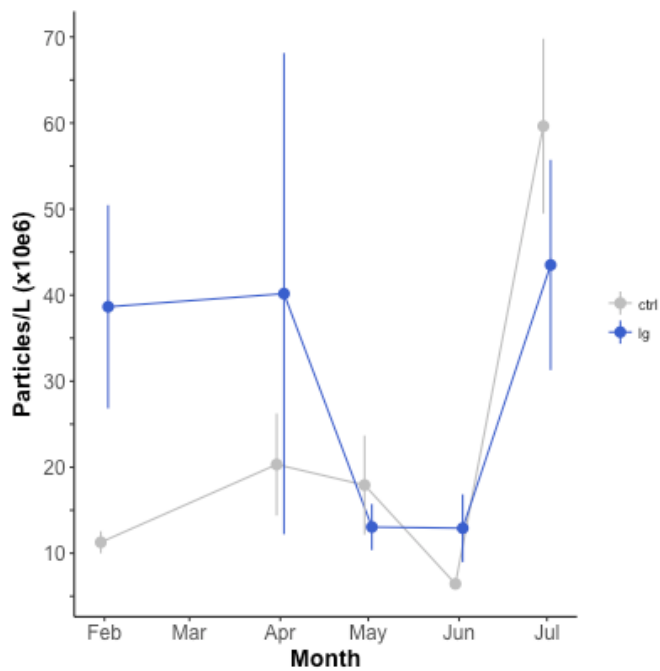


Figure 9: Particle number concentration, in million particles per liter. Particle number concentration was suppressed in May compared to July, with variability in June between treatments (sm-CeO₂, lg-CeO₂, no-Ce).

4. Discussion

4.1 Cerium Mass Balance

Despite theories surrounding Stoke's law, there was no significant difference in the mass of cerium in surface water due to the size of nanoceria dosed. Moreover, both treatments were significantly different from the control, further suggesting that size does not affect nanoceria aquatic fate even in the presence of natural nanoparticles.

Large peaks of total Ce in the water column and the associated variability between triplicate treatments were observed a few times over nine months [Fig.5]. Uneven distribution of nanoceria in surface water could explain the error, where the aliquots analyzed are not representative. The error between triplicates could also highlight heterogeneity between mesocosm environments. Some aquatic variables limit aggregation and thus aid in suspension, like low ionic strength, high dissolved organic matter, or degree of algal bloom. Since samples were not filtered, precautions for algae were taken, but avoidance was not guaranteed. Further work on correlations with aquatic measurands characterization should illuminate or eliminate these theories.

Egeria contained more cerium in mesocosms treated with sm-CeO₂ than other treatments. Ratio of Ce in rinsed and unrinsed (mg/mg) *Egeria* for each treatment was not consistent. Lg-CeO₂ treated *Egeria* had a ratio of ~0.5, whereas sm-CeO₂ was ~0.75. These differing ratios highlight the increased internalization of sm-CeO₂ by *Egeria*, and the universal adsorption of nanoceria onto its surfaces or associated periphyton.

Elevated root concentrations for sm-CeO₂ indicate nanoparticle uptake from the sediment environment, and insignificant Ce levels in stems paired against an elevated stovepipe concentration suggest accumulation in *Egeria* its leaves.

Only a small fraction of the 0.75mg nanoceria dosed over the experiment is recovered in the surface water and *Egeria*. Lg-CeO₂ treated mesocosms had $0.6 \pm 0.9\%$ and $1 \pm 0.6\%$ of the 750mg Ce added in surface water and *Egeria*, respectively. Sm-CeO₂ mesocosms had $0.8 \pm 0.4\%$ in surface water and $4 \pm 0.6\%$ in *Egeria*. Accumulation in another environmental compartment is inevitable, especially with the evident accumulation of Ce in roots.

4.2 Applicability of Single Particle ICP-MS

Size detection has challenged the application of spICP-MS to the mesocosm treatments. With the average diameter of sm-CeO₂ well below size detection limit, accurate measurement was impossible from the start, but aggregate measurement was still probable. The water from sm-CeO₂ dosed mesocosms produced a noisy background signal, resulting in an elevated BED each month. Because nanoceria does not dissolve easily, this noise was attributed to large concentration of sm-CeO₂ particles in the spICP-MS analysis. Dilution of the sample could mitigate problem and enable analysis aggregates of sm-CeO₂ particles, but dilution also has the potential to change the aggregation state of the nanoparticles in ways that would not be quantifiable.

The relative high background in the sm-CeO₂ treatments means that comparison of the single particle ICP-MS data between the two size treatments is not appropriate. The high background caused by the sm-CeO₂ noise means setting a higher background signal cutoff (I_B) than for the control or lg-CeO₂ mesocosm. As such, many small particles are removed with a background subtraction, leading to overestimation of average particle mass. I_B is also assumed constant, which may not be the case. Nanoceria particles could be inconsistently elevated during the instrument runtime, but an average collective subtraction of I_B in Eq. 2 could over- or under- estimate the larger aggregates intensities (I_p).

This increase in particle number suggests a disproportionate number of sm-CeO₂ remaining in the water column, especially when accounting for the high BED. However, no conclusions can be made, nor does the total metal data corroborate a significant difference in total cerium in the water column. The elevation in sm-CeO₂ mesocosms also corresponds to an elevated BED, both suggesting an underestimation of particle number and an inaccurate measurement due to background noise [Fig. 7].

Lg-CeO₂ stock solutions appear to lose much of its smaller mass particles once introduced to mesocosm water. The BEDs of those samples are low, this loss is not due to instrument limitations like the sm-CeO₂ samples. Those smaller particles are most likely aggregating and creating larger particle signals. Control natural nanoparticles

exhibit similar lower bounds to their particle distributions, indicating similar aggregation conditions.

5. Conclusions

Lack of size effect on nanoceria retention in surface water suggests a shift in research away from homoaggregation studies. The plethora of other reactive surfaces within a freshwater system outcompetes the potential for homoaggregation. Instead, further investigation into heteroaggregation or agglomeration and into those compartments of nanoceria fate is advised. With size dependent biological uptake, studies into long term effects and mechanisms of uptake should be pursued to better understand the environmental risk of nanoceria. Research on nanoparticle burial and aging would be valuable, as it is assumed to be the predominant fate of nanoceria.

From this study, it is apparent that another technique besides spICP-MS needs to be used to supplement concentration data in nanoceria environmental studies. Realistically, the environment will receive nanoceria inputs from multiple sources, and consequently include many different size NPs. The resulting multimodal, polydisperse particle distribution entering the environment cannot be captured by spICP-MS, and requires a more advanced technique, higher resolution, or better data processing to be able to account for small particle noise.

Appendix A

Sample Collection

Steven Anderson and Marie Simonin, Dept. Of Biology, Duke University

Label acid-washed HDPE (or acid-washed and autoclaved polypropylene) 250 ml bottles. With cap on bottle, submerge bottle horizontally until mouth is 10 cm below the surface. Uncap slightly and fill with about 50 ml and then recap before removing from the water. Shake and then dump this rinse water at the shallow end of the mesocosm and recap the bottle. Submerge the bottle again and uncap, turning the bottle vertically while filling and maintaining the bottle mouth at 10 cm below the water surface. Recap while under water, then store in a cooler on ice until returning to the lab. Pipette 9.5 ml from the *Sampling bottle* into 15mL Centrifuge tube labeled *Unfiltered metals* and preserve by acidifying them with 500 μ l (5% of sample) concentrated HNO₃ and store in dark on the lab bench. Pipette 10ml from *Sampling bottle* into 15mL centrifuge tube labeled *Single Particle*, and store in refrigerator.

Appendix B

Mesocosm Sample Acid Digestion Protocol

Steven Anderson and Marie Simonin, Dept. Of Biology, Duke University

This protocol is intended to work with all solid mesocosm samples, including plants, tissues, and soils.

1. As necessary, prepare your sample. This includes drying, cutting, grinding, etc.
2. Collect a known mass of solid samples.
 - a. This is generally 75 mg of tissue, 250 mg for soils, also depending on the size of your digestion vessel
3. Add concentrated HNO₃ and 30% H₂O₂ in the ratio 2:1
4. Allow to predigest overnight at room temperature
5. Digest by raising to 100°C over 30 minutes, hold for 10 minutes, and allow to cool
6. Dilute to volume using ultrapure water such that HNO₃ is between 1-5%.

Appendix C

Dosing Procedure

Steven Anderson + Marie Simonin, Dept. Of Biology, Duke University

The four treatments are dosed weekly/chronically with the designated NP stock (Au, Cu, and large or small Ce).

In the field, fill the appropriate bottle ~90% of the way with water from the mesocosm to be dosed. Pipette or pour the desired nanomaterial stock into the bottle and affix cap. Mix and invert the bottle over the mesocosm so that the long plastic tube is held just below the water's surface. Slowly move the bottle around the mesocosm so that the NP suspension is released evenly throughout the mesocosm, taking care that the tip of the tube is always below the water's surface. When the bottle appears empty, remove the cap and rinse several times into the mesocosm. Dose all boxes of one treatment before moving on to the next treatment.

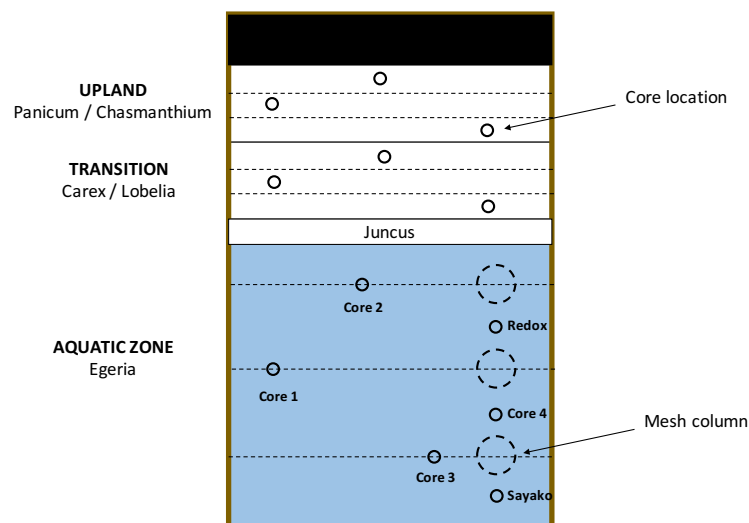
Wait 2hrs before taking a post water sample from all boxes that have been treated with nanoparticles.

Appendix D

Mesocosm sampling plan

Steven Anderson + Marie Simonin, Dept. Of Biology, Duke University

1. Place sediment cores (Aquatic, Transition, Upland) with the drilled cap on the top. Collect the aquatic cores (n=5 or 6).
2. Start collecting Transition and Upland Plant biomass.
3. Collect un-Rinsed (1st) and Rinsed (2nd) Stove pipe Egeria samples + collect extra-floc with Turkey baster (1 bottle per treatment)
4. Collect all Egeria biomass from mesocosm, Clip the roots and put Egeria biomass into the large transparent bin. Transfer Egeria into a green sieve placed over a white pan, shake and collect invertebrates. Transfer back into large bin and rinse with hose. Transfer Egeria into bag for drying.
5. Collect the Transition (n=3) and upland cores(n=3)



References

1. Doshi, Y. *Cerium Oxide Nanoparticles Market by Application - Global Opportunity Analysis and Industry Forecast, 2014-2022*; 2016.
2. Greenwood, N. N.; Earnshaw, A., *Chemistry of the Elements (2nd Edition)*. Elsevier: pp 1227-1249.
3. Mogensen, M.; Sammes, N. M.; Tompsett, G. A., Physical, chemical and electrochemical properties of pure and doped ceria. *Solid State Ionics* **2000**, *129* (1-4), 63-94.
4. Reed, K.; Cormack, A.; Kulkarni, A.; Mayton, M.; Sayle, D.; Klaessig, F.; Stadler, B., Exploring the properties and applications of nanoceria: is there still plenty of room at the bottom? *Environmental Science-Nano* **2014**, *1* (5), 390-405.
5. Klaine, S. J.; Alvarez, P. J. J.; Batley, G. E.; Fernandes, T. F.; Handy, R. D.; Lyon, D. Y.; Mahendra, S.; McLaughlin, M. J.; Lead, J. R., Nanomaterials in the environment: Behavior, fate, bioavailability, and effects. *Environmental Toxicology and Chemistry* **2008**, *27* (9), 1825-1851.
6. Quik, J. T. K.; Lynch, I.; Van Hoecke, K.; Miermans, C. J. H.; De Schampelaere, K. A. C.; Janssen, C. R.; Dawson, K. A.; Stuart, M. A. C.; Van de Meent, D., Effect of natural organic matter on cerium dioxide nanoparticles settling in model fresh water. *Chemosphere* **2010**, *81* (6), 711-715.
7. Sun, C. W.; Li, H.; Chen, L. Q., Nanostructured ceria-based materials: synthesis, properties, and applications. *Energy & Environmental Science* **2012**, *5* (9), 8475-8505.
8. Grulke, E.; Reed, K.; Beck, M.; Huang, X.; Cormack, A.; Seal, S., Nanoceria: factors affecting its pro- and anti-oxidant properties. *Environmental Science-Nano* **2014**, *1* (5), 429-444.
9. Krishnan, M.; Nalaskowski, J. W.; Cook, L. M., Chemical Mechanical Planarization: Slurry Chemistry, Materials, and Mechanisms. *Chemical Reviews* **2010**, *110* (1), 178-204.
10. Speed, D.; Westerhoff, P.; Sierra-Alvarez, R.; Draper, R.; Pantano, P.; Aravamudhan, S.; Chen, K. L.; Hristovski, K.; Herckes, P.; Bi, X. Y.; Yang, Y.; Zeng, C.; Otero-Gonzalez, L.; Mikoryak, C.; Wilson, B. A.; Kosaraju, K.; Tarannum, M.; Crawford, S.; Yi, P.; Liu, X. T.; Babu, S. V.; Moinpour, M.; Ranville, J.; Montano, M.; Corredor, C.; Posner, J.; Shadman, F., Physical, chemical, and in vitro toxicological characterization of nanoparticles in chemical mechanical planarization suspensions used in the semiconductor industry: towards environmental health and safety assessments. *Environmental Science-Nano* **2015**, *2* (3), 227-244.
11. Barton, L. E.; Auffan, M.; Bertrand, M.; Barakat, M.; Santaella, C.; Masion, A.; Borschneck, D.; Olivi, L.; Roche, N.; Wiesner, M. R.; Bottero, J.-Y., Transformation of Pristine and Citrate-Functionalized CeO₂ Nanoparticles in a Laboratory-Scale Activated Sludge Reactor. *Environmental Science & Technology* **2014**, *48* (13), 7289-7296.
12. Limbach, L. K.; Bereiter, R.; Mueller, E.; Krebs, R.; Gaelli, R.; Stark, W. J., Removal of oxide nanoparticles in a model wastewater treatment plant: Influence of agglomeration and surfactants on clearing efficiency. *Environmental Science & Technology* **2008**, *42* (15), 5828-5833.

13. Gomez-Rivera, F.; Field, J. A.; Brown, D.; Sierra-Alvarez, R., Fate of cerium dioxide (CeO₂) nanoparticles in municipal wastewater during activated sludge treatment. *Bioresource Technology* **2012**, *108*, 300-304.
14. Astruc, D., *Nanoparticles and Catalysis*. Wiley: 2008.
15. Park, B.; Donaldson, K.; Duffin, R.; Tran, L.; Kelly, F.; Mudway, I.; Morin, J.-P.; Guest, R.; Jenkinson, P.; Samaras, Z.; Giannouli, M.; Kouridis, H.; Martin, P., Hazard and risk assessment of a nanoparticulate cerium oxide-based diesel fuel additive - A case study. *Inhalation Toxicology* **2008**, *20* (6), 547-566.
16. Skillas, G.; Qian, Z.; Baltensperger, U.; Matter, U.; Burtscher, H., The influence of additives on the size distribution and composition of particles produced by diesel engines. *Combustion Science and Technology* **2000**, *154*, 259-273.
17. Batley, G. E.; Halliburton, B.; Kirby, J. K.; Doolette, C. L.; Navarro, D.; McLaughlin, M. J.; Veitch, C., Characterization and ecological risk assessment of nanoparticulate CeO₂ as a diesel fuel catalyst. *Environmental Toxicology and Chemistry* **2013**, *32* (8), 1896-1905.
18. Gantt, B.; Hoque, S.; Willis, R. D.; Fahey, K. M.; Delgado-Saborit, J. M.; Harrison, R. M.; Erdakos, G. B.; Bhave, P. V.; Zhang, K. M.; Kovalcik, K.; Pye, H. O. T., Near-Road Modeling and Measurement of Cerium-Containing Particles Generated by Nanoparticle Diesel Fuel Additive Use. *Environmental Science & Technology* **2014**, *48* (18), 10607-10613.
19. Walkey, C.; Das, S.; Seal, S.; Erlichman, J.; Heckman, K.; Ghibelli, L.; Traversa, E.; McGinnis, J. F.; Self, W. T., Catalytic properties and biomedical applications of cerium oxide nanoparticles. *Environmental Science-Nano* **2015**, *2* (1), 33-53.
20. Celardo, I.; Pedersen, J. Z.; Traversa, E.; Ghibelli, L., Pharmacological potential of cerium oxide nanoparticles. *Nanoscale* **2011**, *3* (4), 1411-1420.
21. Heckman, K. L.; DeCoteau, W.; Estevez, A.; Reed, K. J.; Costanzo, W.; Sanford, D.; Leiter, J. C.; Clauss, J.; Knapp, K.; Gomez, C.; Mullen, P.; Rathbun, E.; Prime, K.; Marini, J.; Patchefsky, J.; Patchefsky, A. S.; Hailstone, R. K.; Erlichman, J. S., Custom Cerium Oxide Nanoparticles Protect against a Free Radical Mediated Autoimmune Degenerative Disease in the Brain. *Acs Nano* **2013**, *7* (12), 10582-10596.
22. Chen, J. P.; Patil, S.; Seal, S.; McGinnis, J. F., Rare earth nanoparticles prevent retinal degeneration induced by intracellular peroxides. *Nature Nanotechnology* **2006**, *1* (2), 142-150.
23. Zhou, X. H.; Wong, L. L.; Karakoti, A. S.; Seal, S.; McGinnis, J. F., Nanoceria Inhibit the Development and Promote the Regression of Pathologic Retinal Neovascularization in the Vldlr Knockout Mouse. *Plos One* **2011**, *6* (2).
24. Limbach, L. K.; Li, Y. C.; Grass, R. N.; Brunner, T. J.; Hintermann, M. A.; Muller, M.; Gunther, D.; Stark, W. J., Oxide nanoparticle uptake in human lung fibroblasts: Effects of particle size, agglomeration, and diffusion at low concentrations. *Environmental Science & Technology* **2005**, *39* (23), 9370-9376.
25. Lowry, G. V.; Gregory, K. B.; Apte, S. C.; Lead, J. R., Transformations of Nanomaterials in the Environment. *Environmental Science & Technology* **2012**, *46* (13), 6893-6899.

26. Hotze, E. M.; Phenrat, T.; Lowry, G. V., Nanoparticle Aggregation: Challenges to Understanding Transport and Reactivity in the Environment. *Journal of Environmental Quality* **2010**, 39 (6), 1909-1924.
27. Collin, B.; Auffan, M.; Johnson, A. C.; Kaur, I.; Keller, A. A.; Lazareva, A.; Lead, J. R.; Ma, X. M.; Merrifield, R. C.; Svendsen, C.; White, J. C.; Unrine, J. M., Environmental release, fate and ecotoxicological effects of manufactured ceria nanomaterials. *Environmental Science-Nano* **2014**, 1 (6), 533-548.
28. Keller, A. A.; Wang, H.; Zhou, D.; Lenihan, H. S.; Cherr, G.; Cardinale, B. J.; Miller, R.; Ji, Z., Stability and Aggregation of Metal Oxide Nanoparticles in Natural Aqueous Matrices. *Environmental Science & Technology* **2010**, 44 (6), 1962-1967.
29. Van Koetsem, F.; Verstraete, S.; Van der Meeren, P.; Du Laing, G., Stability of engineered nanomaterials in complex aqueous matrices: Settling behaviour of CeO₂ nanoparticles in natural surface waters. *Environmental Research* **2015**, 142, 207-214.
30. Quik, J. T. K.; Stuart, M. C.; Wouterse, M.; Peijnenburg, W.; Hendriks, A. J.; van de Meent, D., Natural colloids are the dominant factor in the sedimentation of nanoparticles. *Environmental Toxicology and Chemistry* **2012**, 31 (5), 1019-1022.
31. Cornelis, G.; Ryan, B.; McLaughlin, M. J.; Kirby, J. K.; Beak, D.; Chittleborough, D., Solubility and Batch Retention of CeO₂ Nanoparticles in Soils. *Environmental Science & Technology* **2011**, 45 (7), 2777-2782.
32. Velzeboer, I.; Quik, J. T. K.; van de Meent, D.; Koelmans, A. A., RAPID SETTLING OF NANOPARTICLES DUE TO HETEROAGGREGATION WITH SUSPENDED SEDIMENT. *Environmental Toxicology and Chemistry* **2014**, 33 (8), 1766-1773.
33. Liu, X. T.; Chen, K. L., Aggregation and interactions of chemical mechanical planarization nanoparticles with model biological membranes: role of phosphate adsorption. *Environmental Science-Nano* **2016**, 3 (1), 146-156.
34. Buettner, K. M.; Rinciog, C. I.; Mylon, S. E., Aggregation kinetics of cerium oxide nanoparticles in monovalent and divalent electrolytes. *Colloids and Surfaces a-Physicochemical and Engineering Aspects* **2010**, 366 (1-3), 74-79.
35. Tella, M.; Auffan, M.; Brousset, L.; Morel, E.; Proux, O.; Chaneac, C.; Angeletti, B.; Pailles, C.; Artells, E.; Santaella, C.; Rose, J.; Thiery, A.; Bottero, J. Y., Chronic dosing of a simulated pond ecosystem in indoor aquatic mesocosms: fate and transport of CeO₂ nanoparticles. *Environmental Science-Nano* **2015**, 2 (6), 653-663.
36. Tella, M.; Auffan, M.; Brousset, L.; Issartel, J.; Kieffer, I.; Pailles, C.; Morel, E.; Santaella, C.; Angeletti, B.; Artells, E.; Rose, J.; Thiery, A.; Bottero, J. Y., Transfer, Transformation, and Impacts of Ceria Nanomaterials in Aquatic Mesocosms Simulating a Pond Ecosystem. *Environmental Science & Technology* **2014**, 48 (16), 9004-9013.
37. Auffan, M.; Masion, A.; Labille, J.; Diot, M. A.; Liu, W.; Olivi, L.; Proux, O.; Ziarelli, F.; Chaurand, P.; Geantet, C.; Bottero, J. Y.; Rose, J., Long-term aging of a CeO₂ based nanocomposite used for wood protection. *Environmental Pollution* **2014**, 188, 1-7.

38. Baalousha, M.; Ju-Nam, Y.; Cole, P. A.; Gaiser, B.; Fernandes, T. F.; Hriljac, J. A.; Jepson, M. A.; Stone, V.; Tyler, C. R.; Lead, J. R., Characterization of cerium oxide nanoparticles-Part 1: Size measurements. *Environmental Toxicology and Chemistry* **2012**, *31* (5), 983-993.
39. Baalousha, M.; Ju-Nam, Y.; Cole, P. A.; Hriljac, J. A.; Jones, I. P.; Tyler, C. R.; Stone, V.; Fernandes, T. F.; Jepson, M. A.; Lead, J. R., Characterization of cerium oxide nanoparticles-Part 2: Nonsize measurements. *Environmental Toxicology and Chemistry* **2012**, *31* (5), 994-1003.
40. Montano, M. D.; Olesik, J. W.; Barber, A. G.; Challis, K.; Ranville, J. F., Single Particle ICP-MS: Advances toward routine analysis of nanomaterials. *Analytical and Bioanalytical Chemistry* **2016**, *408* (19), 5053-5074.
41. Laborda, F.; Jimenez-Lamana, J.; Bolea, E.; Castillo, J. R., Critical considerations for the determination of nanoparticle number concentrations, size and number size distributions by single particle ICP-MS. *Journal of Analytical Atomic Spectrometry* **2013**, *28* (8), 1220-1232.
42. Mitrano, D. M.; Ranville, J. F.; Bednar, A.; Kazor, K.; Hering, A. S.; Higgins, C. P., Tracking dissolution of silver nanoparticles at environmentally relevant concentrations in laboratory, natural, and processed waters using single particle ICP-MS (spICP-MS). *Environmental Science-Nano* **2014**, *1* (3), 248-259.
43. Olesik, J. W.; Gray, P. J., Considerations for measurement of individual nanoparticles or microparticles by ICP-MS: determination of the number of particles and the analyte mass in each particle. *Journal of Analytical Atomic Spectrometry* **2012**, *27* (7), 1143-1155.
44. Bustos, A. R. M.; Petersen, E. J.; Possolo, A.; Winchester, M. R., Post hoc Interlaboratory Comparison of Single Particle ICP-MS Size Measurements of NIST Gold Nanoparticle Reference Materials. *Analytical Chemistry* **2015**, *87* (17), 8809-8817.
45. Reed, R. B.; Higgins, C. P.; Westerhoff, P.; Tadjiki, S.; Ranville, J. F., Overcoming challenges in analysis of polydisperse metal-containing nanoparticles by single particle inductively coupled plasma mass spectrometry. *Journal of Analytical Atomic Spectrometry* **2012**, *27* (7), 1093-1100.
46. Lee, S.; Bi, X. Y.; Reed, R. B.; Ranville, J. F.; Herckes, P.; Westerhoff, P., Nanoparticle Size Detection Limits by Single Particle ICP-MS for 40 Elements. *Environmental Science & Technology* **2014**, *48* (17), 10291-10300.
47. Lowry, G. V.; Espinasse, B. P.; Badireddy, A. R.; Richardson, C. J.; Reinsch, B. C.; Bryant, L. D.; Bone, A. J.; Deonaraine, A.; Chae, S.; Therezien, M.; Colman, B. P.; Hsu-Kim, H.; Bernhardt, E. S.; Matson, C. W.; Wiesner, M. R., Long-Term Transformation and Fate of Manufactured Ag Nanoparticles in a Simulated Large Scale Freshwater Emergent Wetland. *Environmental Science & Technology* **2012**, *46* (13), 7027-7036.
48. Pace, H. E.; Rogers, N. J.; Jarolimek, C.; Coleman, V. A.; Higgins, C. P.; Ranville, J. F., Determining Transport Efficiency for the Purpose of Counting and Sizing Nanoparticles via Single Particle Inductively Coupled Plasma Mass Spectrometry. *Analytical Chemistry* **2011**, *83* (24), 9361-9369.